6

Interaction Between Pulsed Laser and Materials

Jinghua Han[1] and Yaguo Li[2,3]
[1]*College of Electronics & Information Engineering, Sichuan University, Chengdu,*
[2]*Fine Optical Engineering Research Center, Chengdu,*
[3]*Department of Machine Intelligence & Systems Engineering, Akita Prefectural University, Yurihonjo,*
[1,2]*China*
[3]*Japan*

1. Introduction

The research on laser-matter interaction can bridge the gap between practical problems and applications of lasers, which offers an important way to study material properties and to understand intrinsic microstructure of materials. The laser irradiation-induced effects on materials refer to numerous aspects, including optical, electromagnetic, thermodynamic, biological changes in material properties. The laser-matter interaction is an interdisciplinary and complicated subject [1]. When the material is irradiated with lasers, the laser energy will be firstly transformed into electronic excitation energy and then transferred to lattices of materials through collisions between electrons and lattices. The deposition of laser energy will produce a series of effects, such as temperature rise, gasification and ionization. The physical processes of interactions between lasers and matters can be grouped into linear and nonlinear responses of materials to laser pulses, namely thermal effects, nonlinear interactions, laser plasma effects and so forth [2,3]. This chapter aims at analyzing the above-mentioned major effects due to laser irradiation.

2. Thermodynamics

Laser ablation entails complex thermal processes influenced by different laser parameters, inclusive of laser pulse energy, laser wavelength, power density, pulse duration, etc (Fig. 1). According to the response of material to incident laser, the responses can be categorized into two groups: thermal and mechanical effects. Thermal effects refer to melting, vaporization (sublimation), boiling, and phase explosion while mechanical response involves deformation and resultant stress in materials. Different thermal processes will induce different mechanical responses, which will be detailed in the following.

2.1 Thermal effects

Materials subjected to laser irradiation will absorb the incident laser energy, raising the temperature and causing material expansion and thermal stress in materials. When the stress exceeds a certain value, the material may fracture and/or deform plastically. Material expansion will induce various changes in refractive index, heat capacity, etc.

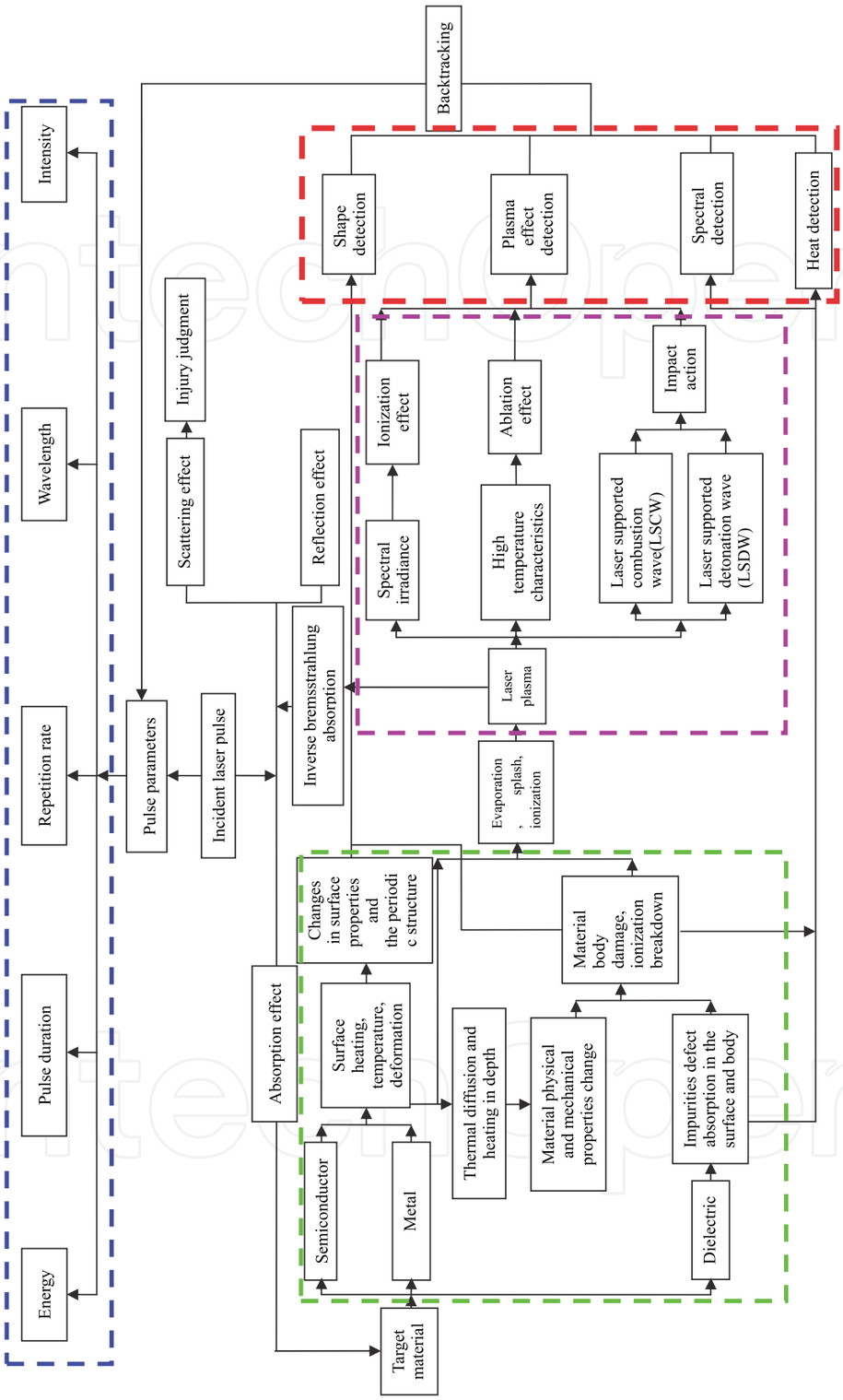

Fig. 1. Laser-matter interactions involve numerous complicated processes, inclusive of physical, mechanical, thermal, optical effects, etc. A full understanding of laser-matter interactions continues to be elusive.

The deposition of the laser pulse energy can heat the materials and raise the temperature of materials. Given that laser beam is perpendicular to the surface of materials (flat surface), the temperature with respect to time t and depth x will be:

$$\Delta T(x,t) = 2(1-R)\alpha I_0 \frac{t}{\pi k \rho C} ierfc \frac{x}{2\sqrt{kt/\rho C}} \tag{2.1}$$

where, t is the laser pulse irradiation time, R is the reflectivity, α is the absorptivity, I_0 is the spatial distribution of laser intensity, k is thermal conductivity, ρ is the density of irradiated materials. When $x > 4\sqrt{kt/\rho C}$, the surface temperature will be simplified as:

$$\Delta T(t) = \frac{2\alpha I_0 \sqrt{t}}{\sqrt{\pi k \rho C}} \tag{2.2}$$

The temperature rise may alter physical and optical properties of materials. The influence of temperature rise will be discussed in more detail.

A Analysis of damage threshold

If the laser energy level at which the irradiated materials start to melt is referred to as the damage threshold (LIDT) of the materials, it is clear that the LIDT is directly proportional to $\sqrt{\tau}$ as shown in Eqt. (2.2). A number of experiments evidence that for laser pulses that τ >10ps, the proportional relationship is applicable to vast majority of semiconductor materials, metals, and dielectric thin films coated on optical components, etc. However, the damage threshold increases with decreasing pulse duration for the laser pulses <10ps. The variation is due to different damage mechanisms of materials when subjected to ultra-short laser pulses[4], since the heat diffusion does not accord with the Fourier's heat conduction law.

B Thermal distortion and stress in solid-state lasers

Materials can absorb the energy of the incident laser, a part of which will be converted into heat. Non-uniform temperature distribution will appear because of the uneven heat

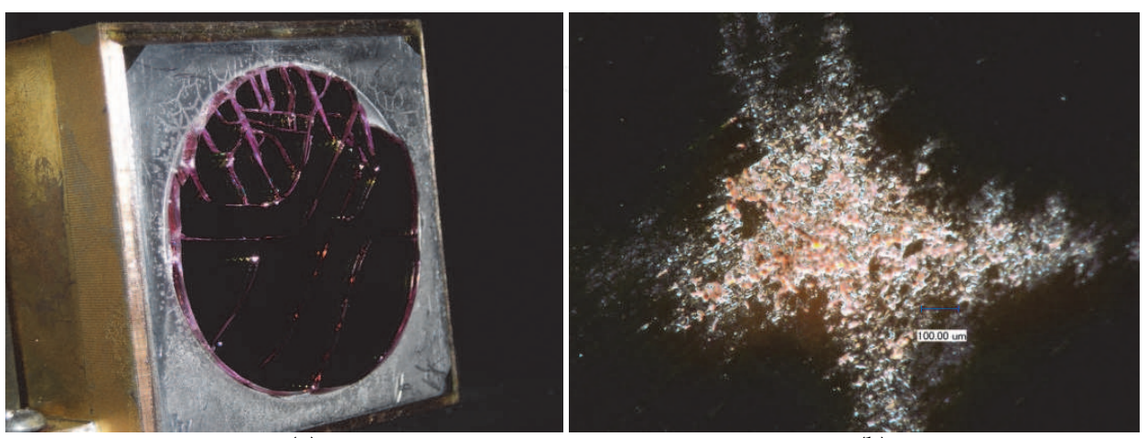

(a) (b)

Fig. 2.1. Thermal fractures of Nd:YAG and melting of SiO_2 thin film coated on Nd:YAG in a high-energy laser (Courtesy of Dr. Huomu Yang)

diffusion. Consequently, expansion and contraction will lead to laser-induced thermal stress. The stress can limit the average workable power of solid-state lasers (Fig. 2.1). Thermo-aberration can seriously affect the uniformity of the output laser field and therefore induce the phase distortion (Fig. 2.2).

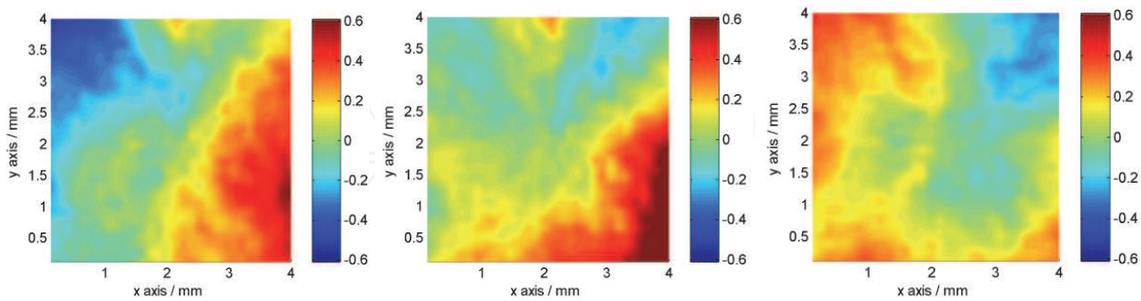

(a)original (b) irradiated for 15min (c) distortion

Fig. 2.2. The distorted wavefront in laser heated K9 glass (The wavelength was 635nm and Shack Hartmann sensor was used to record the wavefront distortion. Courtesy of Dr.Yongzhao Du)

C Frequency doubling

The deposition of laser pulse energy can result in thermal depolarization in optical crystals for doubling/tripling frequency and also degrade the efficiency of frequency doubling. Self-thermal-effect resulting from pump loss will influence the harmonic conversion of the incident laser.

During the process of harmonic conversion, crystals inevitably absorb the energy of fundamental frequency light and frequency-doubled/tripled light. Part of the absorbed energy will convert into heat leading to uniform temperature rise in crystals, which will give rise to a refractive index ellipsoid and disturb phase matching. Furthermore, harmonic conversion efficiency will drop and the quality of output beam will deteriorate [5].

2.2 Melting and solidification

With the increase of laser pulse energy, materials will absorb more laser energy and the deposited energy will cause the material to melt in the case that materials temperature

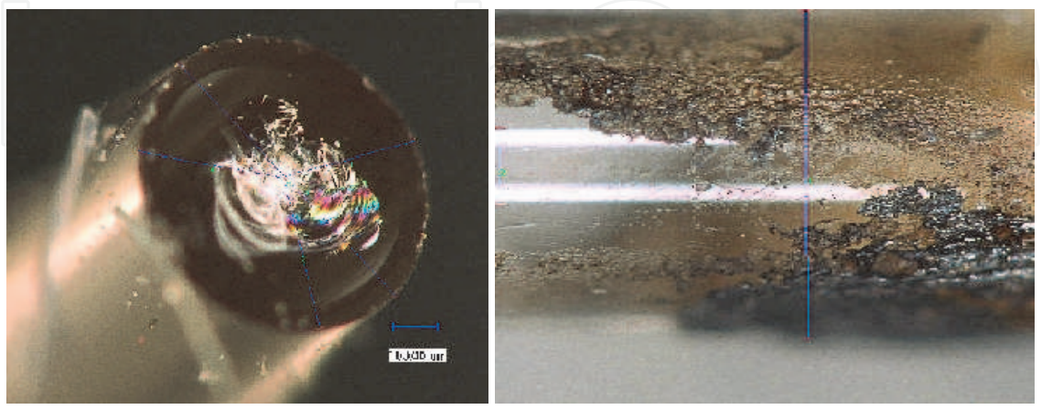

Fig. 2.3. Morphologies of melting damage on the end surface of end-pumped fiber laser. The material is continuously heated with repetitive pumped laser pulses and finally damaged due to non-uniform thermal stress. (Courtesy of Dr. Xu Han)

exceeds the melting point (Fig. 2.3). Melting followed by solidification will change the atomic structure of materials and can realize the mutual transformation between crystalline and amorphous state.

2.3 Ionization and gasification

Laser-induced gasification can be divided into surface gasification and bulk gasification. As the temperature continues to increase to the vaporization point, part of the absorbed laser energy is converted into the latent heat of evaporation, the kinetic energy of gasification and the quality of spray steam. With increasing the laser intensity, the melted materials will be gasified and/or ionized. The gasification is discussed based mainly on liquid-gas equilibrium. Gaseous particles with the Maxwell distribution will splash out from the molten layer. The gasified particles are ejected several microns away from the surface. The space full of particles is the so-called Knudsen layer.

The ionization will greatly enhance the absorption and deposition of the laser energy. After ionization is completed, the inverse bremsstrahlung absorption dominates the absorption of plasma. Re-crystallization of the ionized materials may cause changes in material structure. The damage of SiO_2 thin film coated on $LiNbO_3$ crystal is taken as an example (Fig. 2.4):

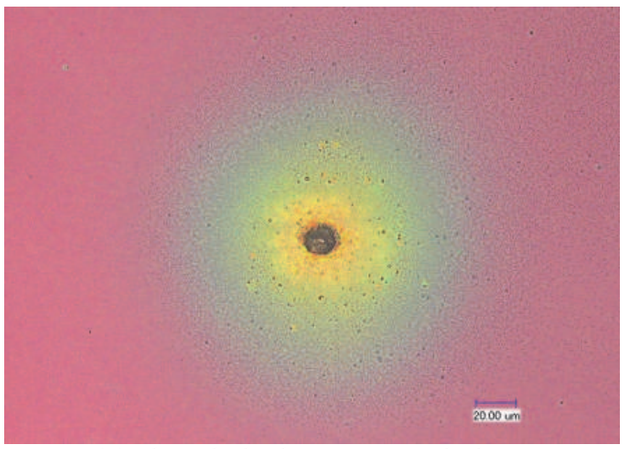

(a) The whole damage morphology

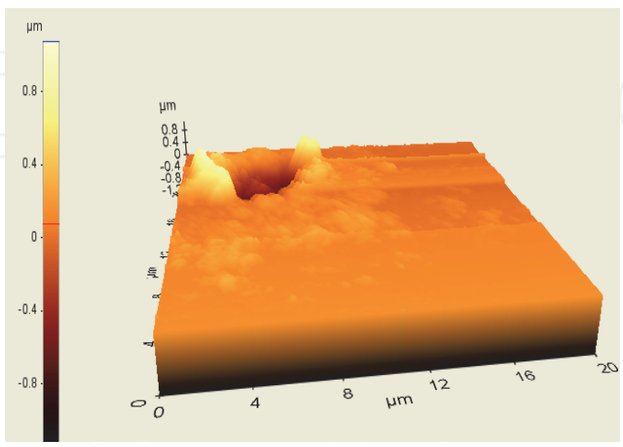

(b) The micro-morphology of a crater

Fig. 2.4. Damage morphologies of laser induced SiO_2 thin film. (Courtesy of Ms. Jin Luo)

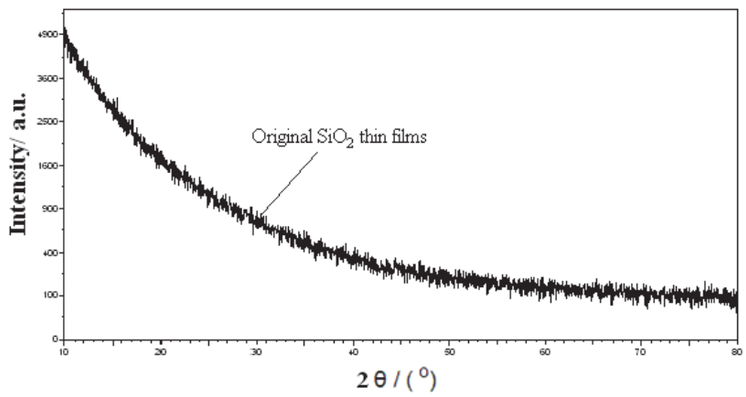

(a) Original SiO_2 thin film

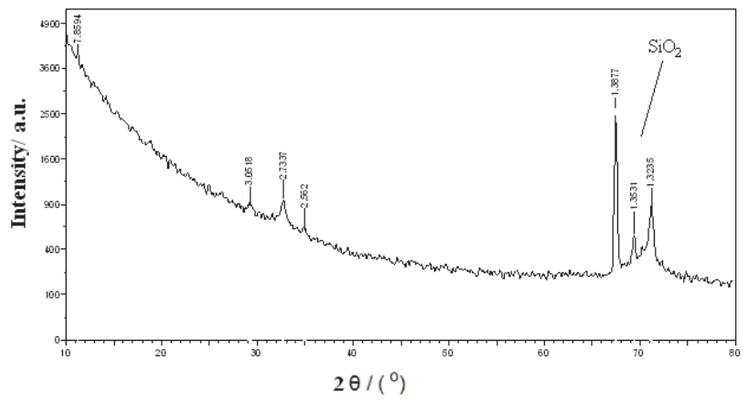

(b) Damaged SiO_2 thin film

Fig. 2.5. The XRD spectra of SiO_2 thin films on lithium niobate crystal (Courtesy of Dr. Ruihua Niu)

Figure 2.5 (a) shows that the film without being damaged is amorphous in that no diffraction peaks appear in the XRD spectrum whilst several apparent peaks are apparent in Fig. 2.5 (b), indicating the appearance of crystalline silica. It can be concluded that ionization can cause material to be re-crystallized.

2.4 Phase explosion

Phase explosion is another important thermal effect. The occurrence of phase explosion follows the stages: the formation of super-heated liquid owing to laser energy deposition; then the generation and growth of nucleation in super-heated liquid and explosion of nucleation.

The physical process is depicted in Fig. 2.6. Upon the irradiation of laser, the temperature of materials will rise and the deposited energy diffuses into the bulk of materials to a certain depth (Figure 2.6(a)); the temperature of melted materials sharply increase to over the boiling point due to the heavy deposition of laser energy; nevertheless, the boiling does not start and the liquid is super-heated because of the absence of nucleation (Figure 2.6(b)); the disturbance will bring about nucleation and the super-heated liquid thickens as the size and the number of bubbles grow (Figure 2.6(c)); the startling boiling will arise once the size of bubbles is sufficiently large and afterwards the super-heated liquid and particles will be ejected. This way, the phase explosion takes place.

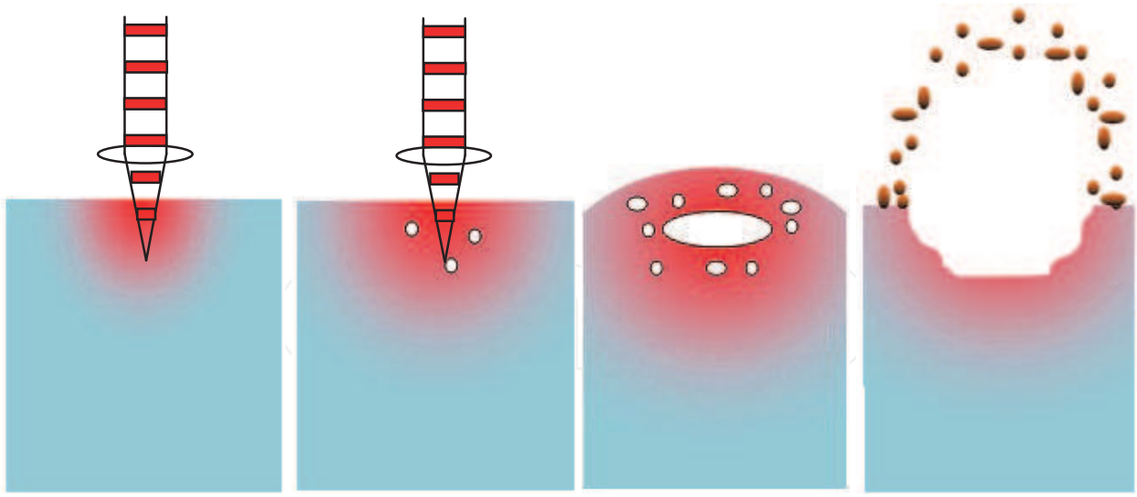

(a) (b) (c) (d)

Fig. 2.6. The generation of phase explosion

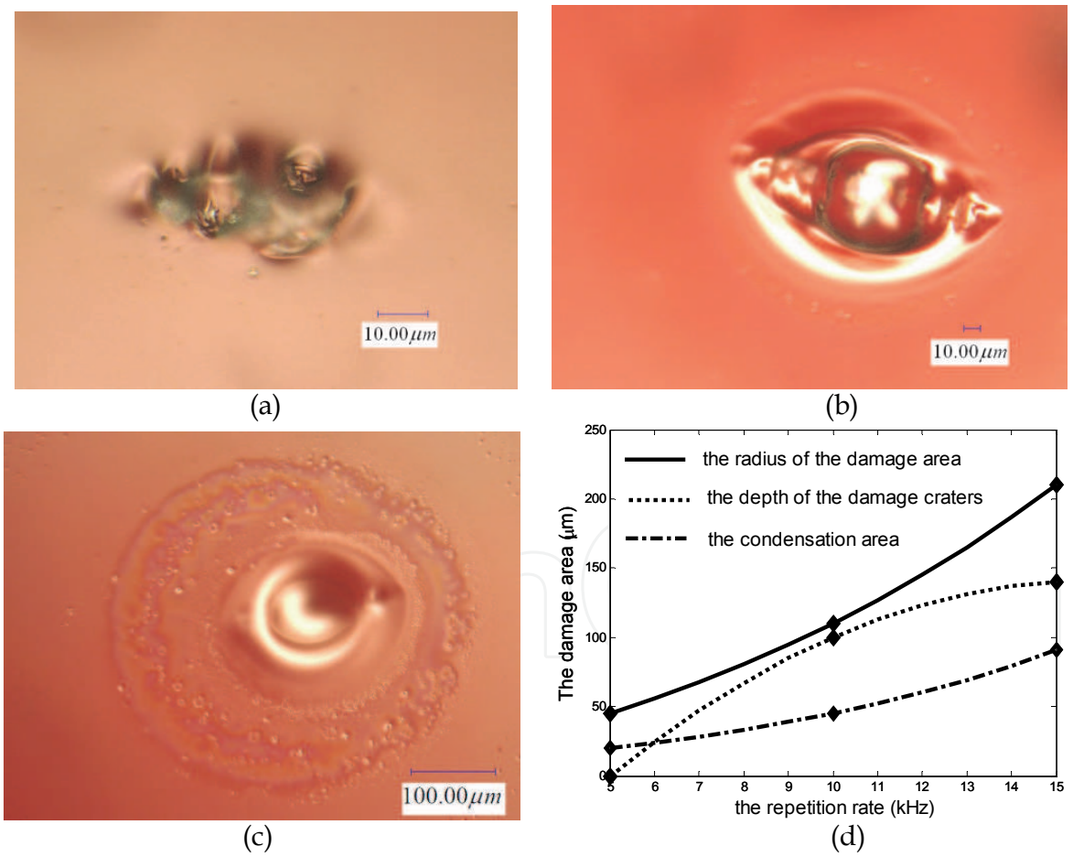

(a) (b) (c) (d)

Fig. 2.7. The damage morphology induced by different repetition rate laser pulses. (a) The damage morphology induced by pulses with repetition rate of 5 kHz. (b) The damage morphology induced by pulses with repetition rate of 10 kHz. (c) The damage morphology induced by pulses with repetition rate of 15 kHz. (d) The dependence of the depth, size and of the damaged craters on the repetition rate.

In order to generate phase explosion, three requirements must be met: 1. the fast creation of super-heated liquid, the temperature of which should at least be (0.8-0.9) Tcr (Tcr is the critical temperature) [6]; 2. the thickness of super-heated liquid is large enough to accommodate the nuclear, usually on the order of tens of microns; 3. sufficient time t_c during which the size of nucleation reaches the critical size r_c, generally several hundreds of picoseconds. All the three factors are indispensable [7]. The generation of phase explosion requires specific laser pulses and material properties. The power density of laser pulses should be more than the threshold of materials (~10^{10}W/cm^2).

The phase explosion can be generated not only by single pulse but also by high-repetition rate pulses [8]. Shown below are the morphologies of craters damaged with pulses of different repetition rates (pulse energy Q= 42.7μJ, total pulse number N = 3.6 × 10^6) 5 kHz, 10 kHz and 15 kHz, respectively (Fig. 2.7).

(a) Phase explosion damage (b) The center of the depression pit (c) Molten zone and the microparticles

Fig. 2.8. Damage morphology induced by phase explosion (15kHz)

Fig.2.8(a) through 2.8(c) present the damage morphologies of materials exposed to high-repetition pulsed laser. There exists successively micro-size particles populated region and melting region from the center of the crater. Numerous micro-granules can be seen in the melting region. The set of pictures imply that the material was damaged due to phase explosion induced by the high-repetition-rate pulsed laser.

3. Effects of nonlinear interaction

Irradiated by high-intensity laser, the material exhibits a variety of nonlinear effects, such as self-focusing, multi-photon ionization, avalanche ionization, etc. The following analyzes the processes of small-scale self-focusing and nonlinear ionization.

3.1 Nonlinear ionization

When the laser beam of low energy is incident onto transparent material, linear absorption happens alone. The electrons in valence band will absorb incident laser and transit from bound states to free states when materials are irradiated with high energy lasers, which is referred to as nonlinear ionization containing two different modes: photo-ionization and avalanche ionization.

The band gap in dielectrics is wide and a single photon is not able to induce ionization and the material cannot directly absorb incident laser of low intensity. Photo-ionization consists

of multi-photon ionization (MPI) and tunnel ionization: if the electric field is strong enough to make the electrons overcome potential barrier and ionize, the ionization is called tunnel ionization; multi-photon ionization is the process that the electron absorbs more photons at a time to gain enough energy beyond potential trap and to be ionized.
The Keldysh parameter can be used to classify multi-photon ionization and tunnel ionization, depending on the frequency and intensity of the incident laser and material band-gap[9].

$$\gamma = \frac{\omega}{e}\left[\frac{mcn\varepsilon_0 E_g}{I}\right]^{1/2} \tag{3.1}$$

where, ω is laser frequency, I is the laser intensity at focal point, m is the reduced mass, e is electron charge, c is the speed of light, n is the refractive index, ε_0 is material dielectric constant, E_g is material energy gap.

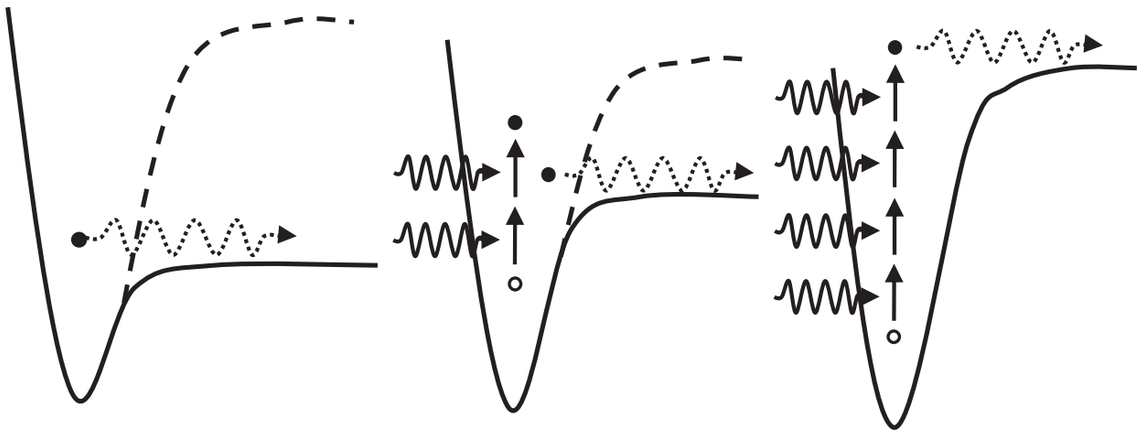

Fig. 3.1. Schematic of photo-ionization for different Keldysh parameters.

As $\gamma > 1.5$ the primary effect is multi-photon ionization; while $\gamma < 1.5$ the main effect is tunnel ionization (Fig.3.1). Both effects should be considered for the transitional state. It also can be seen that when the material is exposed to low frequency and high power laser, tunnel ionization plays the leading role in nonlinear photo-ionization; otherwise, multi-photon ionization is the primary effect.
Conduction band electrons (seed electrons) in material can absorb subsequent photons to raise its energy. When the energy of conduction band electrons rise to a certain degree, the energized electrons can excite electrons in valance band to conduction band through collisions with other valance band electrons and produce a pair of conduction band electrons with lower kinetic energy. The number of conduction band electrons increases exponentially. The above process is the avalanche ionization (Fig. 3.2).
Nonlinear ionization can cause the increase in the density of free electrons which they strongly absorb laser energy, and in turn the density of free electrons increases sharply, which eventually induces the laser plasma and results in breakdown damage.

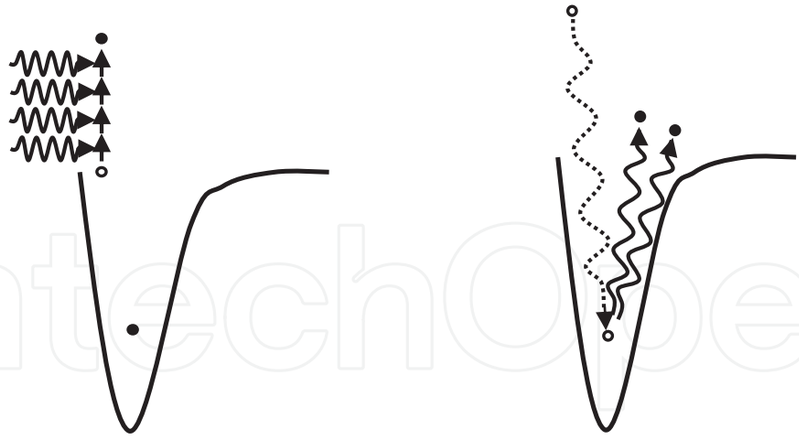

(a) MPI (b) Avalanche ionization

Fig. 3.2. Schematic diagram of the avalanche ionization

3.2 Self-focusing

The refractive index varies accordingly with the increase of the laser density, which can be written as $n = n_0 + n_2 I$, where $I = \frac{1}{2}\varepsilon_0 c n_0 |E|^2$ and $n_2 = \frac{3\chi(3)}{4\varepsilon_0 c n_0^2}$ .The parameter n_2 is related to laser self-focusing and self-phase modulation. When $n_2 > 0$, the medium can be considered a positive lens and self-focusing occurs when the beam travels through the medium; otherwise the defocusing happens. In light of the difference in pulse duration and nonlinear polarization time, self-focusing can be grouped into steady-state self-focusing (continuous wave of invariable amplitude), quasi-steady self-focusing (both field and power are functions of the delayed time), and transient self-focusing (when pulse duration is shorter than or similar to medium response time, the medium response time must be taken into account). In addition, the small scale self-focusing caused by the incident beam with uneven distribution of intensity or irregular modulations can result in beam splitting, medium filamentous damage, and spectrum detuning, etc.

Kerr lens effect is continuously pronounced with increasing the pulse power of laser and self-focusing becomes conspicuous until the laser power approaches the critical power at which a balance is struck between the wave-front bending caused by the diffraction and self-focusing lens. In this way, the light beam will transmit in the form of filament (Fig. 3.3). When self-focusing occurs, the nonlinear ionization can produce laser plasma and lead to filamentous destruction (Fig. 3.4). In addition, the self-defocusing of laser plasma is an obstacle to further self-focusing.

The mechanism of small scale self-focusing has been studied since early 1970s. The classical theory is B-T theory [10]. The B integration characterizes the size of self-focusing damage, which is named after Breakup-integral $B = \left(2\pi/\lambda_0\right)\int \gamma I_0(z)dz$. B integral is a criterion for determining the extent of small scale self-focusing and the causes of additional phase as well as the sources of phase modulation and spectral broadening.

B-T theory remains the basic theory for nonlinear optical transmission. The world's largest high-power solid laser–'National Ignition Facility' (NIF) is designed based on B-T theory [11].

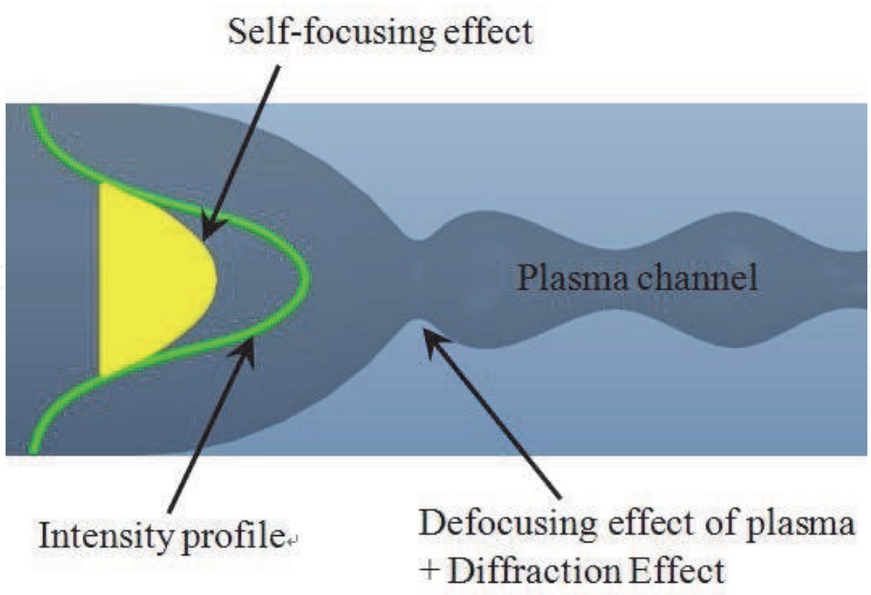

Fig. 3.3. The illustration of self-focusing filaments

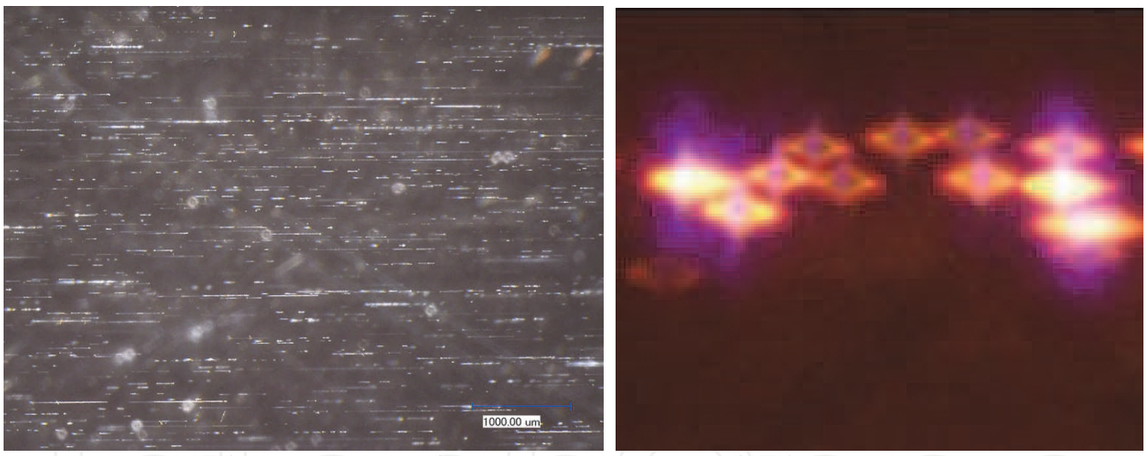

(a)Filaments in crystals (b)Filaments in water

Fig. 3.4. Small-scale self-focusing. (Courtesy of Dr. Ruihua Niu and Dr. Binhou Li)

3.3 Extrinsic damage

Dielectrics have wide band-gap and low absorptive capacity and possess high intrinsic damage threshold. However, the damage factually occurs at the laser intensity several orders of magnitude lower than the intrinsic threshold of materials, which is due mostly to the extrinsic damage. In other words, the impurities of the narrow band gap material can severely lower the damage threshold of dielectrics. When impurities of narrow band gap exist in dielectrics, the impurities can absorb laser strongly and sharply increase energy deposition locally. The rapid deposition of laser energy can result in melting, gasification ionization of dielectrics and laser plasma and therefore local damage (Fig. 3.5).

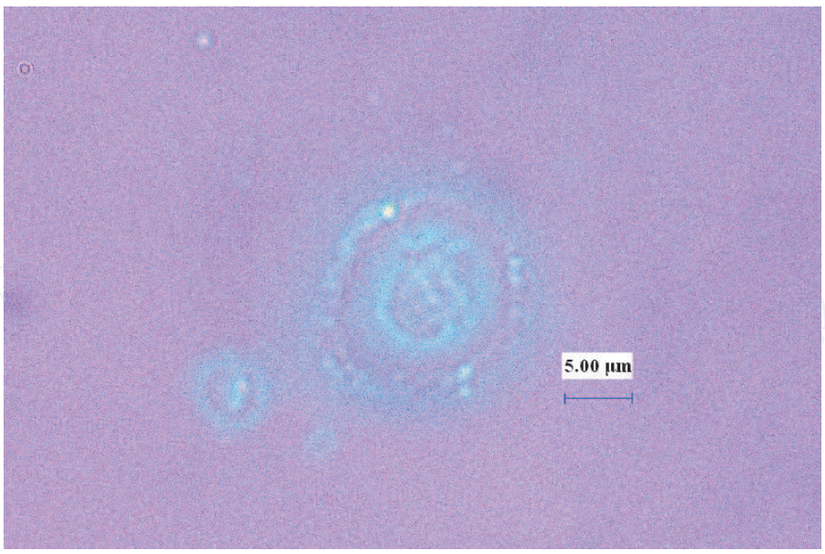

Fig. 3.5. The ripples of SiO_2 antireflection coating due to laser damage

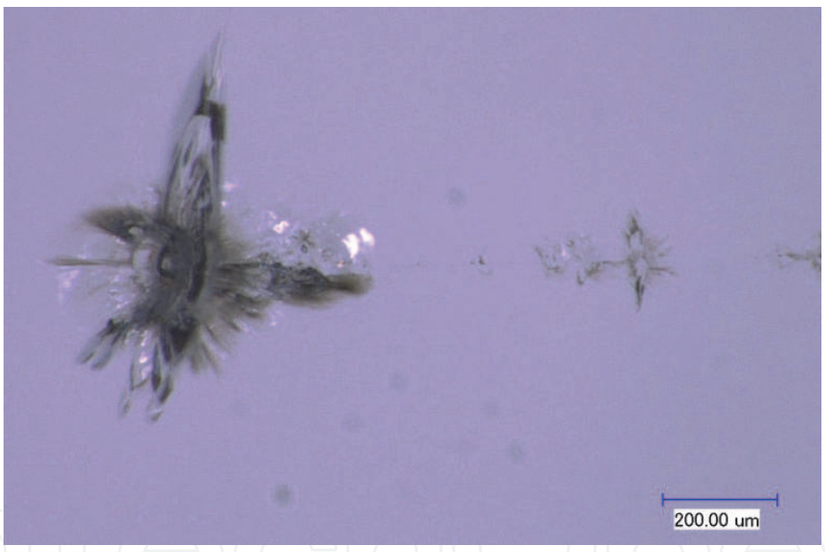

Fig. 3.6. The laser damage in the bulk of K9 glass (1064nm, 13.6ns) (Courtesy of Dr. Guorui Zhou and Dr. Shutong Wang)

The self-focusing filamentous damage in K9 glass is characterized by the connection of filamentous destruction and burst damage caused by particles that strongly absorb the laser energy (Fig. 3.6) [12]. In high-power laser systems, the elimination of platinum inclusions in Nd:Glass is of great importance so as to improve the damage threshold of Nd:glass [13].

4. Laser induced plasma shock wave

4.1 Shock wave formation

As the laser plasma with high temperature and pressure expands outward, shock waves will be formed. In fluid dynamics, the shock wave generated by the blast in early 1930s has

been studied in detail and the point explosion model was proposed. Based on the model of point explosion, zel'dovich and Raiser systematically studied the laser plasma expansion and developed the Sedov-Taylor instantaneous point explosion [14].

Taking into account the lasting time of real explosion, the process of shock wave is considered to consist of two stages.

1. When $t \le \tau_0$, shock wave starts due to the ablation of laser to target materials. High-energy pulsed laser ablates and sputters the target materials to form plasma; the plasma expands immediately and rapidly and forms shock wave. In the meantime, shock wave continues to absorb the laser energy, which keeps expediting the shock waves. When $t = \tau_0$, the speed of shock wave is maximized at the end of laser action. The first stage of the formation of shock wave ends.

$$R(t) = A_0 \left(\alpha E(t)\right)^{1/2+v} t^{2/2+v} \qquad t \le \tau_0 \tag{4.1}$$

where $A_0 = A(\rho_1)^{-1/2+v}$, α is the ratio of the energy transferred to shock waves to the total energy of a laser pulse.

2. When $t > \tau_0$, the stage is characterized with the expansion and propagation of shock waves in the air. It is experimentally proved that shock wave eventually decays into acoustic pulses to propagate in sonic speed in the air.

$$R(t) = A_1 (t - \tau_0) \left(1 - \alpha_0 \exp\left[-k \left(\frac{\tau}{t - \tau_0} \right)^n \right] \right) + R_0 \qquad t > \tau_0 \tag{4.2}$$

where $A_1 = \frac{2A_0}{2+v} \tau_0^{-v/2+v} \left(\alpha E(t)\right)^{1/2+v}$, k, α_0, n are undetermined coefficients.

No more energy is replenished during the propagation of shock wave because the laser irradiation discontinues. Thereby, although the radius of shock wave front keeps increasing, the velocity of shock wave propagation slows down and the intensity of shock wave is dwindling.

4.2 Laser supported absorption wave (LSAW)

Ionized vapor can absorb partial or entire energy of the incident laser to form plasma on the surface, so the temperature and intensity in gasification surface is the highest. A part of plasma expands outwards and the rest is constrained within the light path, which is different from normal gases in motion and referred to as laser supported absorption wave (LSAW) [1].

The plasma is ionized in part by low energy pulses and absorbs partial energy of pulses and the plasma shock wave propagates at the subsonic speed due to thermal conductivity, which is laser supported combustion wave (LSCW). If the laser pulse intensity is increased, the pressure, temperature and velocity of absorption wave increase correspondingly and the absorptivity of wave will be further enhanced and thus the wave consumes most of the laser energy. Then the plasma will contract and plasma propagates at supersonic speed, which is the laser supported detonation wave (LSDW).

The LSDW damaged the target materials seriously due to its exceedingly high temperature and pressure. Assuming that expansion process is isentropic and one-dimensional, the velocity and pressure of plasma wave with respect to target materials can be formulated as [1]:

$$p_2 = p_1[(\gamma+1)/2\gamma]^{2\gamma/(\gamma-1)} \tag{4.3}$$

$$p_1 = \rho_0 u^2/(\gamma+1) \tag{4.4}$$

$$u = [2(\gamma^2-1)I/\rho_0]^{1/3} \tag{4.5}$$

where p_1, $p_2$and u are the pressure of LSDW on the target surface, wave rear pressure of LSDW wave and the expansion rate of LSDW wave front, respectively, ρ_0 is the density of ambient atmosphere , γ is adiabatic coefficient of the plasma, I is the power density of laser on target surface. The temperature also depends on the power density of laser pulses [15]. $T = \alpha_T I^{1/(\beta+4)}$,where α_T and β are constants, I is the power density of incident laser in W/cm^2 .

4.3 Effect of laser plasma spectral irradiance

Laser plasma with a very wide spectrum from ultraviolet to infrared is composed of background continuous spectrum and linear spectrum due to elements including in the plasma. The continuous spectrum of radiation is mainly attributed to bremsstrahlung and recombination radiation process [16]. The bremsstrahlung radiation is the process that the electromagnetic wave is emitted due to the transition of free-state to free-state contributed to the collision between free electrons and ions. The temperature of free electron of plasma descends quickly during the process. Recombination radiation process is the process during which free electrons are captured to be bound-state by ions in electron-ion collision; meanwhile excessive energy is emitted in the form of electromagnetic radiation. The continuous spectrum with shorter wavelength and more significant intensity results from the bremsstrahlung, while the longer can be ascribed to recombination radiation. The laser plasma also has irradiant ionization effects. According to Keldysh ionization theory, the shorter wavelength, the higher the photon energy and the more likely the materials will be ionized; the short wavelength of laser plasma is much shorter than incident laser, so the ionization effect of short wavelength laser is more apparent.

The laser plasma effects act on the materials synergically. As an example, the breakdown of polycrystalline silicon by 1064nm focused laser beam is demonstrated in Fig 4.1. The laser used was 18ns in pulse duration (FWHM) and 500mJ of pulse energy. The focused spot is ~150 microns in diameters.

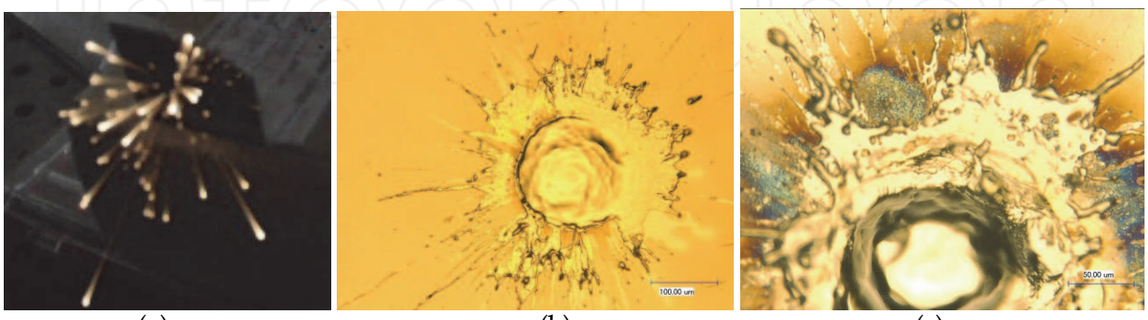

(a) (b) (c)

Fig. 4.1. The laser induced damage in polycrystalline silicon. (a) the sputtering of laser-induced plasma. (b) the damaged area is comprised of a crater and splashed materials. (c) the damage morphology created with 7Hz repetition rate laser for 1s. (Courtesy of Dr. Yanyan Liu)

The process of laser damage can be described by the action of LSDW，ionization，etc. The results are shown as follows (Fig. 4.2).

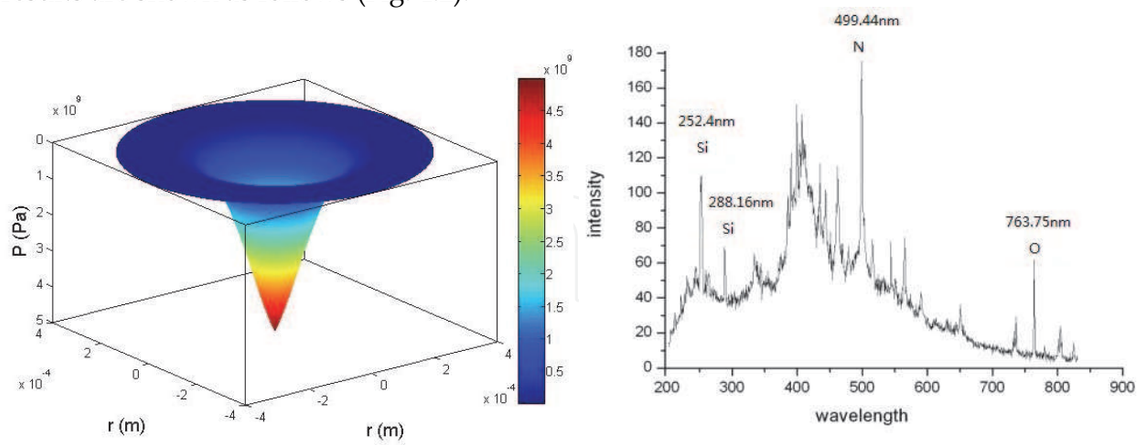

(a) The pressure distribution of LSDW (b) Plasma spectra.

Fig. 4.2. LSDW and laser-induced plasma spectra. (Courtesy of Dr. Lingdong Bao)

The thermal and ionization cause materials to be fully melted and ionized and then the mixture is pushed out by LSDW. The laser plasma enhances material ionization. Thus the comprehensive effects form the damage pit surrounded by cooled material.

5. The femtosecond laser effects

Ultrashort pulse laser distinguished from nanosecond pulse laser lies in its peculiar laser-matter mechanism, supercontiuum generation and color-center accumulation etc. Then we will start with the ultra-short laser-matter mechanism. The ulatrafast laser refers to femtosecond pulsed laser in this chapter unless otherwise specified.

5.1 Mechanism of interaction between femtosecond laser and matters

The pulse duration of femto-second pulse is of the order of 10^{-15}s much shorter than conventional pulsed lasers. The electrons in materials absorb the energy of incident laser and their kinetic energy will increase. The activated electrons transfer energy to lattice by means of electron-lattice collision. This way, the temperature of materials rises. It needs several femtoseconds for electrons to absorb the laser energy (interactions between the photons and electrons) and the time of electron-lattice collision is of the order of picoseconds while lattices of materials melt within several nanoseconds.

There are plenty of free electrons in metals and semiconductors and the laser energy can be deposited by absorbing the energy of photons directly. The laser action process can be formulated with equation [17].

$$\begin{cases} C_e \dfrac{\partial T_e}{\partial t} = K\nabla^2 T_e - g\left(T_e - T_i\right) + A\left(r,t\right) \\ C_i \dfrac{\partial T_i}{\partial t} = g\left(T_e - T_i\right) \end{cases} \tag{5.1}$$

where, C_e、C_I are the heat capacity of electrons and lattices, K the conductivity of materials, A the thermal source relating to laser pulse, g the coefficient of electron-phonon coupling.

The first equation represents the deposition of laser energy to electrons and the other is the coupling of electron energy to lattices.
As to dielectrics with very low free electron density, dielectrics must be ionized by high intensity laser. The ionization effect of femto-second laser on dielectrics can be divided into multiphoton ionization and avalanche ionization. Then ionized electrons can absorb the incident laser energy dramatically; however there is not adequate time for the transferring of energy to lattices and thus the heat diffusion is impossible. By contrast, the energy in nanosecond laser pulses has enough time to be transferred from electrons to lattices, leading to thermodynamic damage.
Speaking generally, the craters created with femtosecond laser are smooth on the edge as compared to nanosecond pulsed lasers (Fig. 5.1). The femtosecond laser damage is more deterministic than ns lasers because of no obvious thermal effects and can be employed to accurately inscribe microstructures[18].

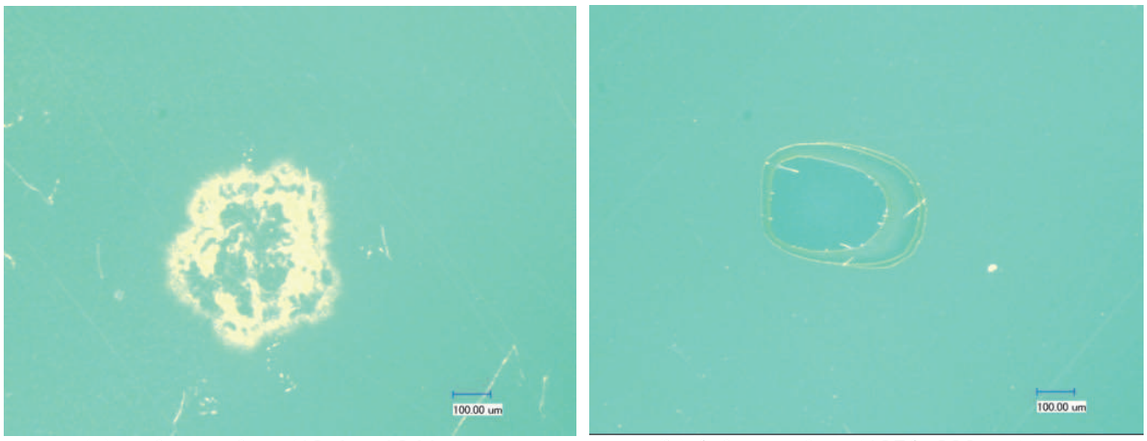

(a) ns laser pluse(13.6ns,1064nm) (b) fs laser pluse(135fs,800nm)

Fig. 5.1. The damage morphologies of SiO_2 thin film induced by nanosecond and fs laser pulse.

5.2 Supercontiuum generation

Supercontinuum generation (SCG) is another important property of fs laser, which belongs to nonlinear optical phenomenon. SCG involves a broad spectrally continuous output when narrow-band incident pulses undergo extreme nonlinear spectral broadening. The SCG has many novel applications in telecommunication, high precision frequency metrology, carrier phase stabilization, medical imaging and pulse compression for its spatial coherence, high brightness, and broad bandwidth [19,20].
The broadband pulse propagation in waveguide can be described by the nonlinear envelope equation. The supercontinuum generation mechanisms includes self-phase modulation (SPM), induced-phase modulation (IPM), crossed-phase modulation (XPM), soliton effects, Raman shift and coupling with dispersive waves, modulation instability, four wave mixing (FWM), the main effects leading to the generation of a broad spectrum starting from a narrow laser line.
The propagation of laser pulse in nonlinear materials can be expressed with nonlinear Schrödinger equation[21]:

$$\frac{\partial E}{\partial z}=\frac{ic}{2n_0\omega_0}(1+\frac{i}{\omega_0}\frac{\partial}{\partial t})^{-1}\nabla_{\perp}^2E-\frac{i}{2}\beta_2\frac{\partial^2E}{\partial t^2}+\frac{\beta_3}{6}\frac{\partial^3E}{\partial t^3}-\frac{i}{24}\beta_4\frac{\partial^4E}{\partial t^4}$$
$$+i\gamma\left[|E|^2E+\frac{i}{\omega_0}\frac{\partial}{\partial t}(|E|^2E)-T_RE\frac{\partial|E|^2}{\partial t}\right]-\frac{\alpha}{2}E \tag{5.2}$$

where, E is the amplitude, c the speed of light, ω_0 the pulse center frequency, n_0 the linear refractive index, β_2 the group velocity dispersion, β_3 third-order dispersion constant, β_4 fourth-order dispersion constant, α the loss coefficient. The first term describes the diffraction and the second, third and fourth terms are material dispersion terms.

There are a variety of nonlinear media that can be used to generate wide supercontinuum, including solids, organic and inorganic liquids and gas [22]. PCF (Photonic crystal fiber) has become an important media to generate wide supercontinuum because of high nonlinearity and low peak power pump threshold (Fig. 5.2).

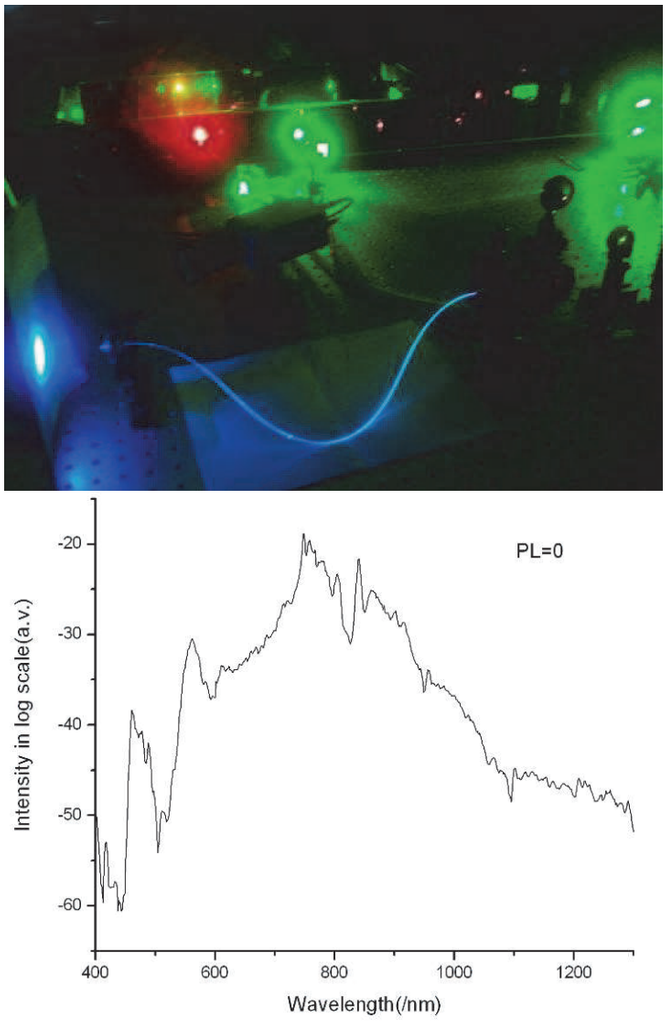

Fig. 5.2. Photonic crystal fiber and supercontinuum spectrum. (Courtesy of Dr. Ping Ying and Dr. Zairu Ma)

5.3 Color centers

Laser induced color center is a major type of material fatigue. It can be reduced by fs laser with high intensity or ns laser pulse with shorter wavelength. The color centers in materials will form if the electron-hole pairs ionized by laser are captured by defects or impurities.

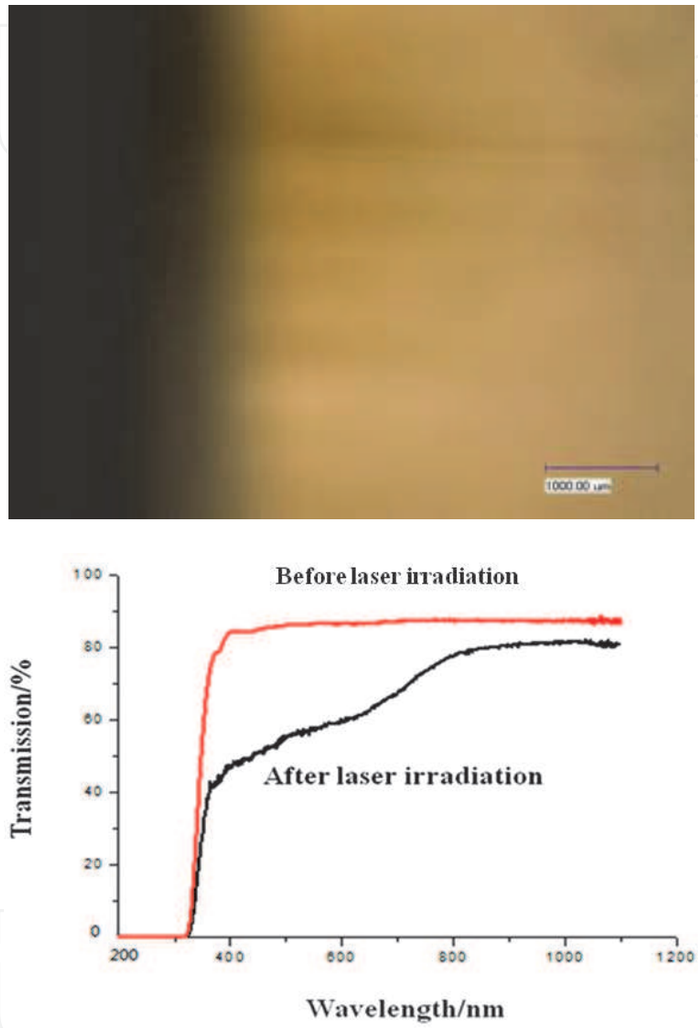

Fig. 5.3. Femtosecond laser induced darkening and transmission spectrum in K9 glass

The figures 5.3 & 5.4 show the grey tracking and corresponding absorption spectra in K9 glass and KTP crystals induced by high-repetition laser pulses with wavelength of 335nm, pulse duration of 13.6ns.

The absorption spectra exhibit several absorption peaks. The absorption at 475 nm is due to charge transferring transitions in Ti^{3+}–Ti^{4+} pairs[1], and the other two are due to the Jahn-Teller effect[23]. For UV ns pulse, free electrons generated by single-photon ionization are the main cause for color centers; in contrast, for fs laser, it is due to multiphoton ionization and avalanche ionization.

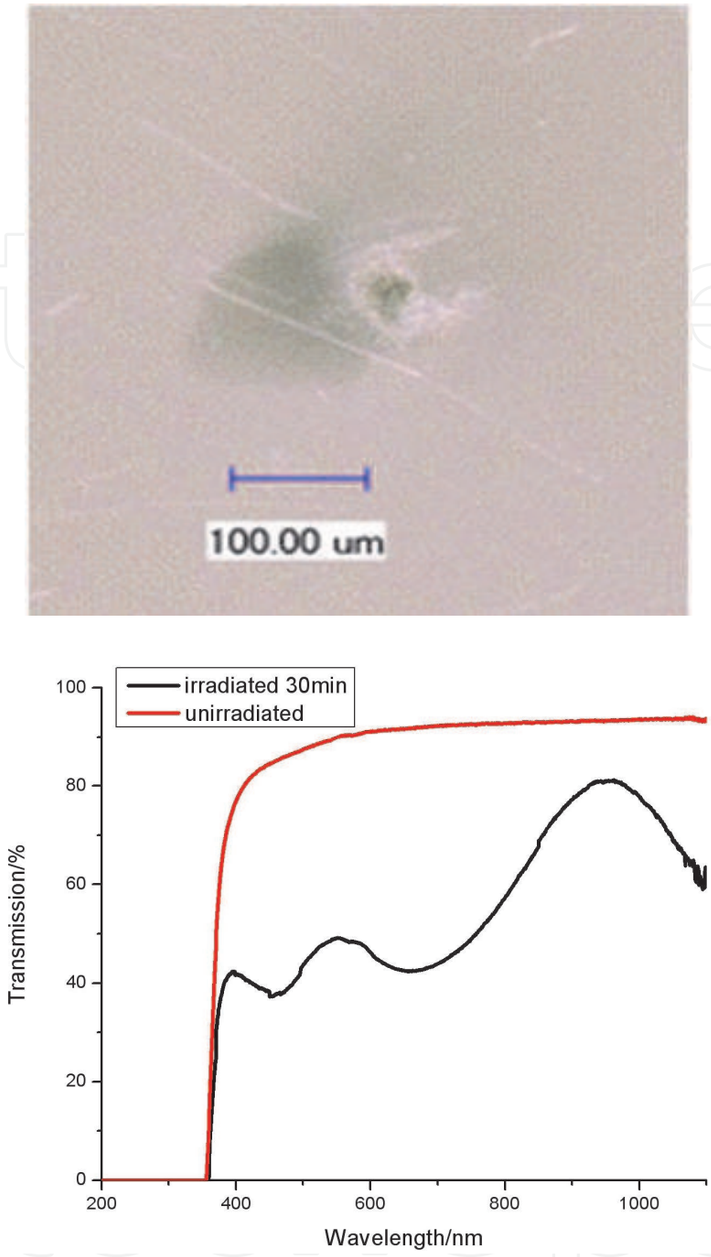

Fig. 5.4. Gray tracking in KTP crystal by 355nm laser radiation for 30min. and the transmission spectra (Courtesy of Dr. Qiuhui Zhang and Dr. Xiang Gao)

5.4 Microstructure induced by femtosecond

Irradiated by ultra-short pulse, semiconductor or metal surface can form a variety of micro and nano-scale structures. The micro-structures are influenced greatly by the laser pulse parameters, such as laser pulse number, pulse wavelength, pulse energy as well as the different external conditions (vacuum, liquid, air)[25,26].We conducted preliminary experiments on the surface periodic structure in silicon induced by repetitive femtosecond pulses, which are in the air or water, and the results obtained are as follows (Fig. 5.5):

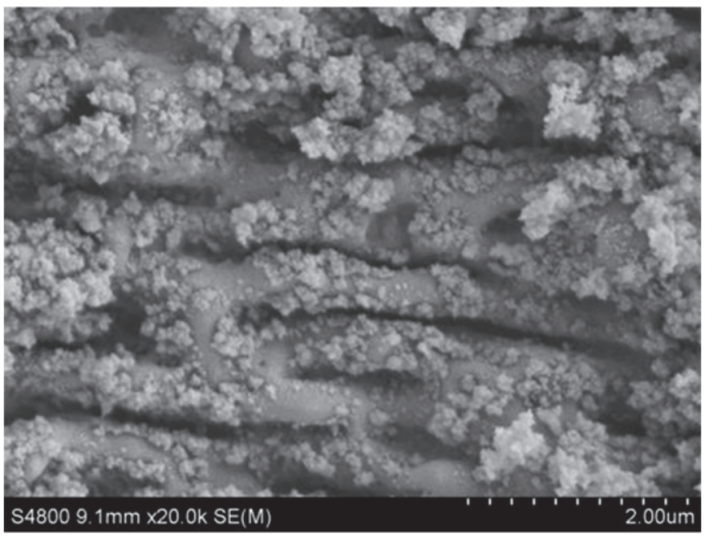

(a)

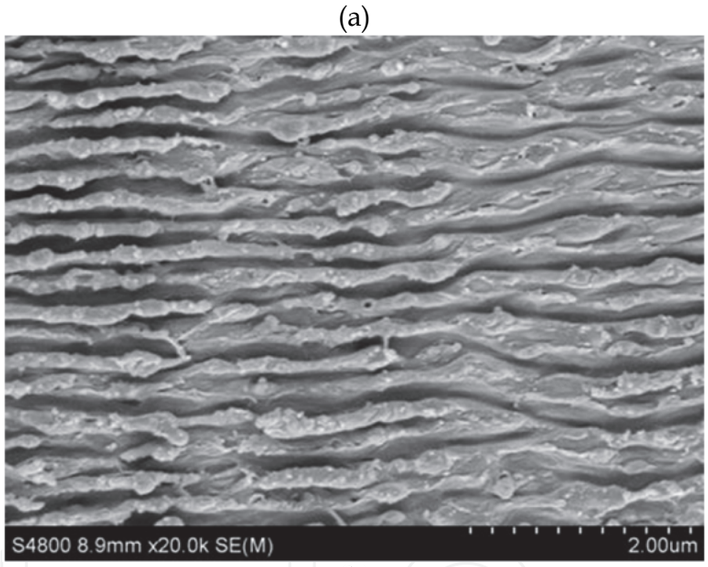

(b)

Fig. 5.5. Periodic structure on the Si surface produced in the air (a) and water (b), respectively with femtosecond pulse (repetitive rate 10Hz, single pulse energy 1mJ,pulse duration 35 fs, 500 pulses).

The study manifests that micro and nano-scale structure are due to the interference of the incident light with the scattered light and/or plasma wave, while nano-particles result from the melting and phase explosion from the shock wave.

6. Acknowledgements

This work was financed by the National Natural Science Foundation of China (Grant No. 60890203 and 10676023) and the Young Faculty Research Fund of Sichuan University (Grant No. 2009SCU11008).

7. References

[1] M. von Allmen and A. Blatter, *Laser-Beam Interactions with Materials: Physical Principles and Applications*, 2nd Edition, Springer-Verlag, Berlin & Heidelberg, Germany, 1995.

[2] R. M. Wood, *Laser-induced damage of optical materials*, IOP Publishing Ltd., London, UK, 2003.

[3] N. Bloembergen, "Laser-induced electric breakdown in solids," IEEE J. Quantum. Electron. 10, 375-386, 1974.

[4] B. C. Stuart, M. D. Feit, S. Herman, A. M. Rubenchik, B. W. Shore, and M. D. Perry, "Nanosecond-to-femtosecond laser-induced breakdown in dielectrics," Phys. Rev. B 53, 1749-1761, 1996.

[5] H. Wang and A. M. Weiner, "Efficiency of short-pulse type-I second-harmonic generation with simultaneous spatial walk-off, temporal walk-off, and pump depletion," IEEE J. Quant. Electron. 39, 1600-1618, 2003.

[6] D. Bleiner and A. Bogaerts, "Multiplicity and contiguity of ablation mechanisms in laser-assisted analytical micro-sampling," Spectrochimica Acta Part B 61, 421-432, 2006.

[7] J. H. Yoo, S. H. Jeong, R. Greif, and R. E. Russo, "Explosive change in crater properties during high power nanosecond laser ablation of silicon," J. Appl. Phys. 88, 1638-1649, 2000.

[8] J. Han, Y. Li, Q. Zhang, Y. Fu, W. Fan, G. Feng, L. Yang, X. Xie, Q. Zhu, and S. Zhou, "Phase explosion induced by high-repetition rate pulsed laser," Appl. Surf. Sci. 256, 6649-6654, 2010.

[9] L. V. Keldysh, "Ionization in the field of a strong electromagnetic wave," Sov. Phys. JETP 20, 1307-1314, 1965.

[10] V. I. Bespalov and V. I. Tanlanov, "Filamentary structure of light beams in nonlinear media," JETP Lett. 3, 307-310, 1966.

[11] "National Ignition Facility Functional Requirements and Primary Criteria," Lawrence Livermore National Laboratory Report NIF-LLNL-93-058, USA, 1994.

[12] J. O. Porteus and S. C. Seitel, "Absolute onset of optical surface damage using distributed defect ensembles," Appl. Opt. 23, 3796-3805, 1984.

[13] J. H. Campbell and T. I. Suratwala, "Nd-doped phosphate glasses for high-energy/high-peak-power lasers," J. Non-Crystal. Solids 263-264, 318-341, 2000.

[14] Ya. B. Zel'dovich and Yu. P. Raizer, *Physics of Shock Waves and High-Temperature Hydrodynamic Phenomena*, 1966 (in Russian) [edited by W. D. Hayes and R. F. Probstein, Dover Publications, Inc., N.Y., USA, 2002.]

[15] T. X. Phuoc, "An experimental and numerical study of laser-induced spark in air," Opt. Lasers Eng. 43, 113-129, 2005.

[16] G. Bekefi, *Radiation processes in plasmas*, John Wiley & Sons, Inc., N.J., 1966.

[17] C. K. Sun, F. Vallee, L. Acioli, E. P. Ippen, and J. G. Fujimoto, "Femtosecond investigation of electron thermalization in gold," Phys. Rev. B 48, 12365-12368, 1993.

[18] B. N. Chichkov, C. Momma, S. Nolte, F. Von Alvensleben, and A. Tunnermann, "Femtosecond, picosecond and nanosecond laser ablation of solids," Appl. Phys. A 63, 109-115, 1996.

[19] D. J. Jones, S. A. Diddams, J. K. Ranka, A. Stentz, R. S. Windeler, J. L. Hall, and S. T. Cundiff, "Carrier envelope phase control of femtosecond mode-locked lasers and direct optical frequency synthesis," Science 288, 635-639, 2000.

[20] I. Hartl, X. Li, C. Chudoba, R. Ghanta, T. Ko, J. G. Fujimoto, J. K. Ranka, R. S. Windeler, and A. J. Stentz, "Ultrahigh-resolution optical coherence tomography using continuum generation in an air-silica microstructure optical fiber," Opt. Lett. 26, 608-610, 2001.

[21] V. P. Kandidov, O. G. Kosareva, I. S. Golubtsov, W. Liu, A. Becker, N. Akozbek, C. M. Bowden, and S. L. Chin, "Self-transformation of a powerful femtosecond laser pulse into a white-light laser pulse in bulk optical media (or supercontinuum generation)," Appl. Phys. B 77, 149-165, 2003.

[22] J. M. Dudley, G. Genty, and S. Coen, "Supercontinuum generation in photonic crystal fiber," Rev. Mod. Phys. 78, 1135–1184, 2006.

[23] M. N. Satyanarayan, H. L. Bhat, M. R. Srinivasan, P. Ayyub, and M. S. Multani, "Evidence for the presence of remnant strain in grey-tracked $KTiOPO_4$," Appl. Phys. Lett. 67, 2810-2812, 1995.

[24] G. M. Loiacono, D. N. Loiacono, T. McGee, and M. Babb, "Laser damage formation in $KTiOPO_4$ and $KTiQAsO_4$ crystals: Grey tracks," J. Appl. Phys. 72, 2705-2712, 1992.

[25] M. Huang, F. Zhao, Y. Cheng, N. Xu, and Z. Xu, "Origin of Laser-induced Near-Subwavelength Ripples: Interference between Surface Plasmons and Incident Laser," ACS Nano 3, 4062-4070, 2009.

[26] P. Lorazo, L. J. Lewis, and M. Meunier, "Thermodynamic Pathways to Melting, Ablation and Solidification in Absorbing Solids Under Pulsed Laser Irradiation," Phys. Rev. B. 73, 134108, 2006.

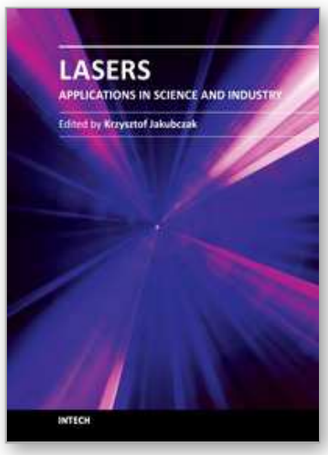

Lasers - Applications in Science and Industry
Edited by Dr Krzysztof Jakubczak

ISBN 978-953-307-755-0
Hard cover, 276 pages
Publisher InTech
Published online 09, December, 2011
Published in print edition December, 2011

The book starts with basic overview of physical phenomena on laser-matter interaction. Then it is followed by presentation of a number of laser applications in the nano-particles and thin films production, materials examination for industry, biological applications (in-vitro fertilization,tissue ablation) and long-range detection issues by LIDARs.

How to reference
In order to correctly reference this scholarly work, feel free to copy and paste the following:

Jinghua Han and Yaguo Li (2011). Interaction Between Pulsed Laser and Materials, Lasers - Applications in Science and Industry, Dr Krzysztof Jakubczak (Ed.), ISBN: 978-953-307-755-0, InTech, Available from: http://www.intechopen.com/books/lasers-applications-in-science-and-industry/interaction-between-pulsed-laser-and-materials

INTECH
open science | open minds

InTech Europe
University Campus STeP Ri
Slavka Krautzeka 83/A
51000 Rijeka, Croatia
Phone: +385 (51) 770 447
Fax: +385 (51) 686 166
www.intechopen.com

InTech China
Unit 405, Office Block, Hotel Equatorial Shanghai
No.65, Yan An Road (West), Shanghai, 200040, China
中国上海市延安西路65号上海国际贵都大饭店办公楼405单元
Phone: +86-21-62489820
Fax: +86-21-62489821

IntechOpen